DETERMINATION OF THE COEFFICIENT OF EDDY VISCOSITY AS A FUNCTION OF HEIGHT AND TIME; AND SEPARATELY AS A FUNCTION OF STABILITY AND VERTICAL SHEAR OF THE WIND

JEREMIAH R. McBRIDE

DETERMINATION OF THE COEFFICIENT OF EDDY VISCOSITY AS A FUNCTION OF HEIGHT AND TIME; AND SEPARATELY AS A FUNCTION OF STABILITY AND VERTICAL SHEAR OF THE WIND

****

Jeremiah R. McBride

DETERMINATION OF THE COEFFICIENT OF EDDY VISCOSITY AS A FUNCTION OF HEIGHT AND TIME; AND SEPARATELY AS A FUNCTION OF STABILITY AND VERTICAL SHEAR OF THE WIND

by

Jeremiah R. McBride
Lieutenant, United States Navy

Submitted in partial fulfillment of
the requirements for the degree of

MASTER OF SCIENCE

IN

METEOROLOGY

United States Naval Postgraduate School
Monterey, California

1960

DETERMINATION OF THE COEFFICIENT OF EDDY VISCOSITY AS A FUNCTION OF HEIGHT AND TIME; AND SEPARATELY AS A FUNCTION OF STABILITY AND VERTICAL SHEAR OF THE WIND

by

Jeremiah R. McBride

This work is accepted as fulfilling
the thesis requirements for the degree of
MASTER OF SCIENCE
IN
METEOROLOGY
from the
United States Naval Postgraduate School

ABSTRACT

A harmonic analysis of the observed diurnal variation of the coefficient of eddy viscosity is conducted at selected levels followed by a mathematical analysis of the amplitude coefficients in order to determine a function of height and time needed to represent this variation. It is found by this approach that a lengthy series of terms, consisting of exponential and polynomial functions of height and trigonometric functions of time and height, would be needed to represent the observed variation.

A two layer empirical model is developed from the observed data which gives the coefficient of eddy viscosity as a function of stability and height in the lower layer, and as a function of vertical shear of the horizontal wind and height in the upper layer.

The author wishes to express his appreciation for the assistance and encouragement of Professors G. J. Haltiner and A. B. Mewborn of the U. S. Naval Postgraduate School in this investigation.

TABLE OF CONTENTS

LIST OF ILLUSTRATIONS

1. Introduction.

In an attempt to account for the observed wind structure in the friction layer, meteorologists have devoted considerable effort to determine the variation of the coefficient of eddy viscosity with respect to time and space.

The layer of frictional influence has been subdivided into the laminar, surface, and spiral layers each possessing certain characteristic properties. The coefficient of eddy viscosity, μ, has been shown to vary linearly with height in the neutral surface layer and as a power function of height in the non-neutral surface layer. Using wind data obtained from double theodolite observations and assuming a steady state, Mildner [6] solved the horizontal equation of motion for μ utilizing finite differences for the derivatives of velocity. He showed that μ increased up to a fairly low elevation in the spiral layer (250 meters) and then decreased to a small residual value near the gradient level.

The Taylor [7] solution for the wind in the spiral layer assumes μ constant, along with a number of other broad assumptions, and yields a general representation of the observed vertical wind variation. More recently, Buajitti and Blackadar [2] and Haltiner [4] have sought the distribution of eddy viscosity as a function of time and height in order to account for the diurnal variations of the wind structure in the friction layer. Haltiner [4] assumes the coefficient of eddy viscosity to have the form

$$K \equiv \mu = g(t)\, k(z)$$

where

$$g(t) = 1 + b\,(\mathrm{Sin}\,\omega t + c\,\mathrm{Sin}\,2\omega t)$$

and k(z) takes on several different exponential forms.

It is the purpose of this investigation to determine the degree of complexity of the function of $\mathcal{M}$ (z, t) needed to yield observed values of $\mathcal{M}$; and also to determine, if possible, the coefficient of eddy viscosity as a function of stability and vertical shear of the wind.

2. The Coefficient of Eddy Viscosity as a Function of Height and Time.

The horizontal equations of motion for turbulent flow where the eddy stresses are assumed to be a function of height and time only and the molecular or viscous stress is considered negligible are

$$\frac{\partial u}{\partial t} + \vec{V}\cdot\nabla u = f(v - v_g) + \frac{1}{\rho}\frac{\partial T_{zx}}{\partial z}$$
$$\frac{\partial v}{\partial t} + \vec{V}\cdot\nabla v = -f(u - u_g) + \frac{1}{\rho}\frac{\partial T_{zy}}{\partial z} \qquad (1)$$

Here T_{zx} and T_{zy} are the components of eddy stress; u_g and v_g the components of the geostrophic wind; $\vec{V}$, the mean wind velocity vector of which u and v are the horizontal components; ρ, the density; and f, the coriolis parameter.

The eddy stresses are assumed to be related to the mean wind shear by the expressions

$$T_{zx} = \mu\frac{\partial u}{\partial z} \qquad T_{zy} = \mu\frac{\partial v}{\partial z} \qquad (2)$$

The geostrophic departure method employs observations of the mean velocity and geostrophic wind to evaluate all the terms of eq (1), so as to yield the distribution of $\frac{\partial T_{zx}}{\partial z}$ and $\frac{\partial T_{zy}}{\partial z}$. This method gives the distribution of stress and eddy viscosity provided the wind components have a maximum at some levels h_x and h_y so that at h_x, $\frac{\partial u}{\partial z} = 0$ and at h_y, $\frac{\partial v}{\partial z} = 0$.

By multiplying eq (1) by ρ and integrating from h_x to an arbitrary height z, the distribution of T_{zx} is obtained. Similarly the distribution of T_{zy} is found. Then eq. (2) leads to two independent estimates of the distribution of eddy viscosity.

$$\mu_x = \frac{\tau_{zx}}{\partial u/\partial z} \qquad \mu_y = \frac{\tau_{zy}}{\partial v/\partial z} \tag{3}$$

Assuming no discrepancies in the procedure or data, $\mu_x = \mu_y > 0$.

Blackadar [1] used the geostrophic departure method on a composite wind distribution obtained by averaging the winds at two stations (Oklahoma City, Oklahoma and Wichita, Kansas) over 24 selected, not necessarily consecutive, one-day periods. Figures 1 and 2, reproduced from Blackadar's [1] data, show the eastward and northward components of the average winds during the 24 day period. Although great care was taken in determining each of the terms of eq (1), Blackadar [1] pointed out that

> "the independent estimates of μ_x and μ_y did not agree and negative values of each were numerous and frequently large. It is assumed that the reason for the poor performance is in the inaccuracy of the geostrophic wind."

For this reason, he devised an indirect method for obtaining the values of u_g and v_g which would minimize the sum of the absolute magnitudes of $\mu_x - \mu_y$ at the four levels (950, 900, 850 and 800 mb). He forced μ_x to be equal to μ_y at a single level and at the two standard radiosonde times; then the geostrophic wind components were computed. Next utilizing the thermal wind relationship and assuming the temperature sounding to be accurate, the values of u_g and v_g were found in the vertical. The variation of geostrophic wind at times other than the standard radiosonde times was determined on the

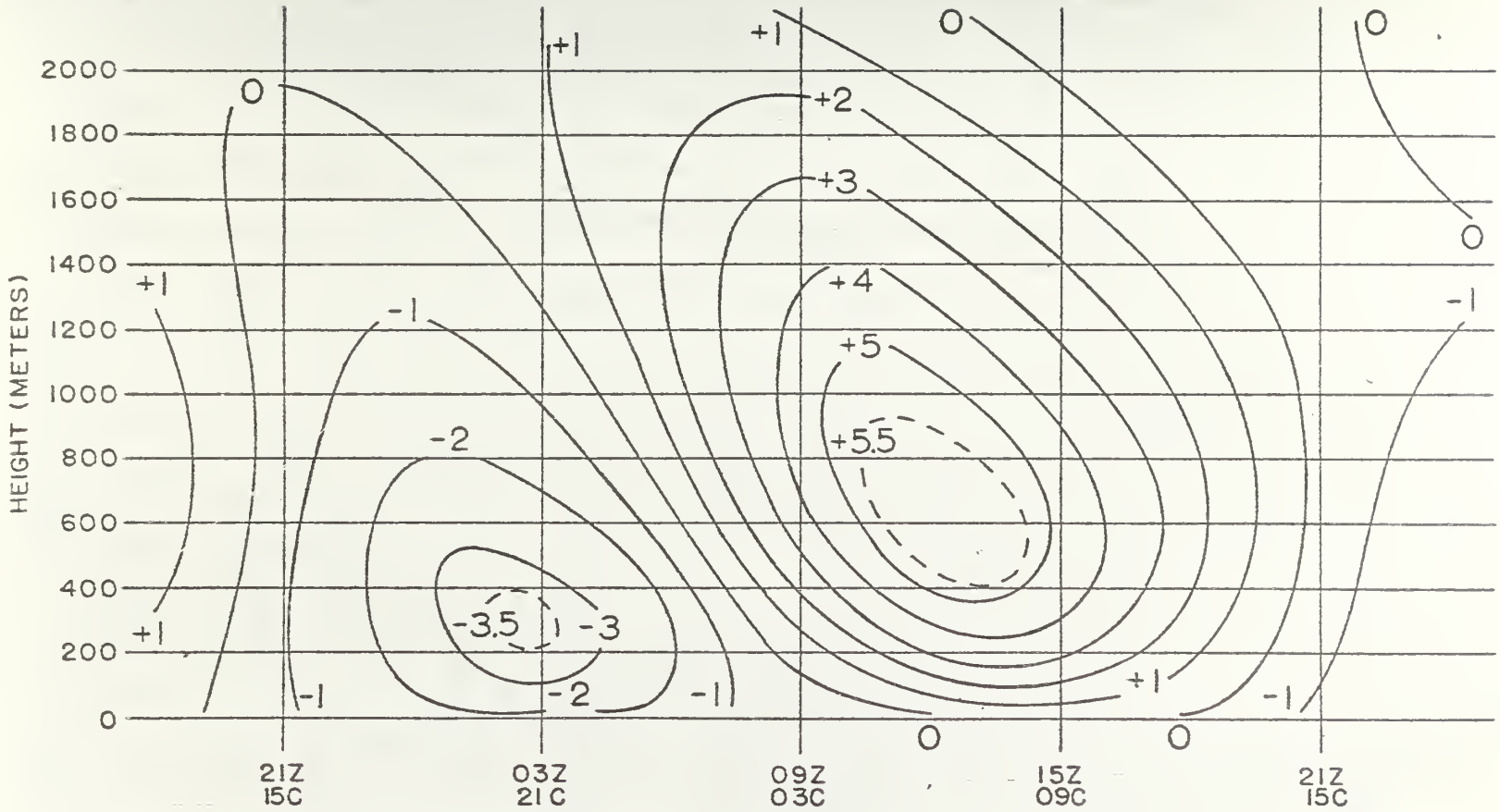

FIG. 1. Eastward component of the average wind at Wichita and Oklahoma City during a 24-day period as a function of height and time. Values are m sec^{-1}, after Blackadar [1].

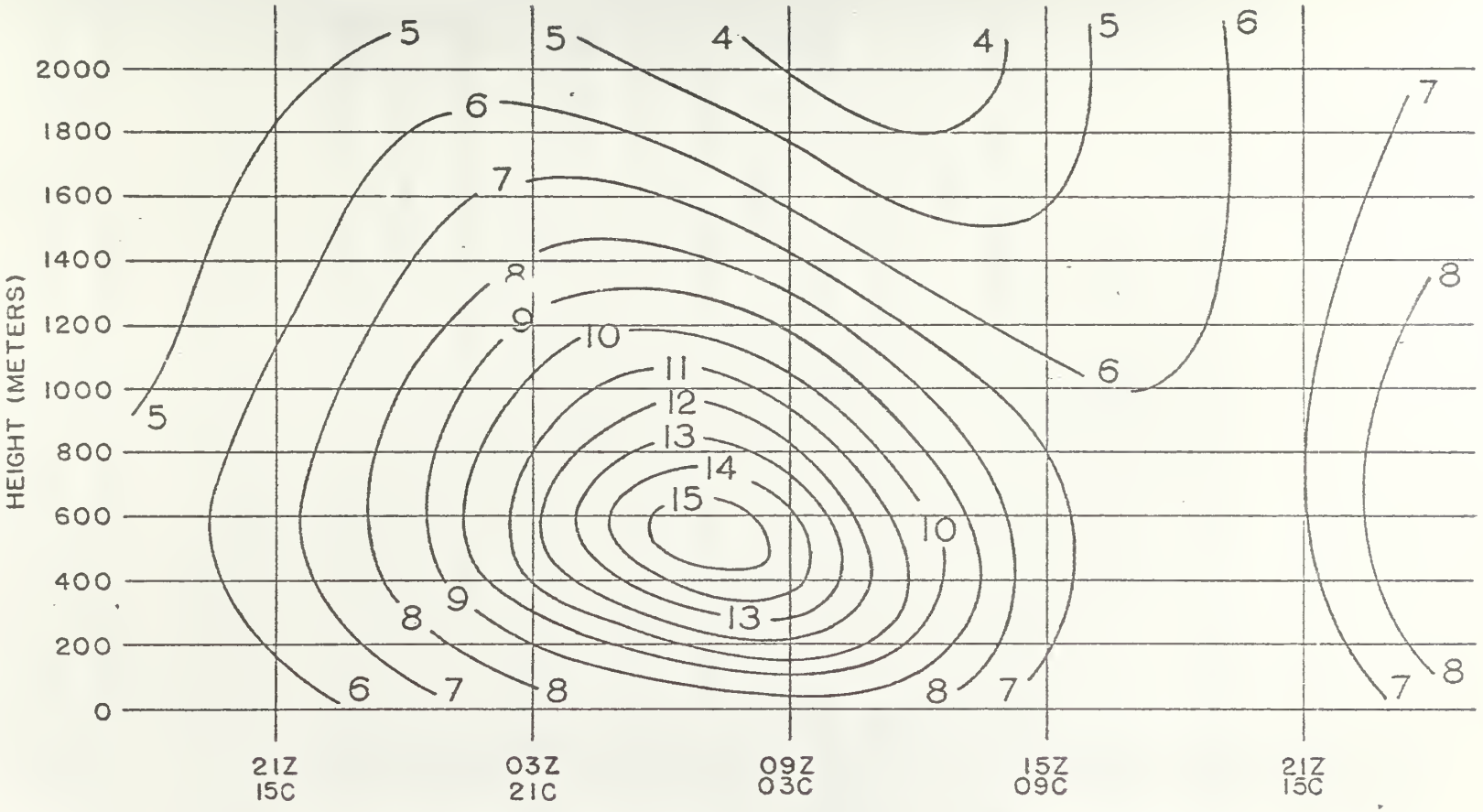

FIG. 2. Northward component of the average wind at Wichita and Oklahoma City during a 24-day period as a function of height and time. Values are m sec^{-1}, after Blackadar[1].

hypothesis that the [illegible] linear function of time. The eddy stresses and eddy [illegible] were then recomputed at 200 meter height intervals and three hourly time intervals. The values of [illegible] and [illegible] so obtained were generally in agreement at all times. Blackadar [1] decided

> "...to dispose of the remaining differences, the best estimate [illegible] was assumed to be given by
>
> [illegible]

Fig. 3 shows Blackadar's [1] computed values of [illegible] as a function of height and time.

It is desired to find a function [illegible] (z,t) which will yield these values of [illegible]. Due to the periodic nature of the solution, fig. 3 must be modified in order to show the same values of [illegible] for corresponding heights at the beginning and end of the 24 hour period. The alteration of fig. 3 was minimized insofar as possible, and the modified fig. 3 is shown as fig. 4.

The following approach to the problem was used. Determine the time series which fits the observed values of [illegible] for 12 times (2 hour intervals) at each of the given heights 0, 200, 400, 600.... 1800 meters. An example for the height of 200 meters is

$$\text{[illegible]}\,2 = \text{[illegible]}(2,t) = A_0(2) + A_1(2)\cos\left[(t + T_1(2)\right] + A_2(2)\cos\left[(2t + T_2(2)\right] + \ldots A_6\cos\left[(6t + T_6(2)\right] \quad (4)$$

Here sine and cosine terms belonging to the same harmonic have been combined: $A_0(2)$ is the mean value, $A_1(2)$ is the amplitude of the first harmonic, $T_1(2)$ is the phase angle of the first harmonic in degrees and t is time in hours after t = 0. (1500 CST), expressed in

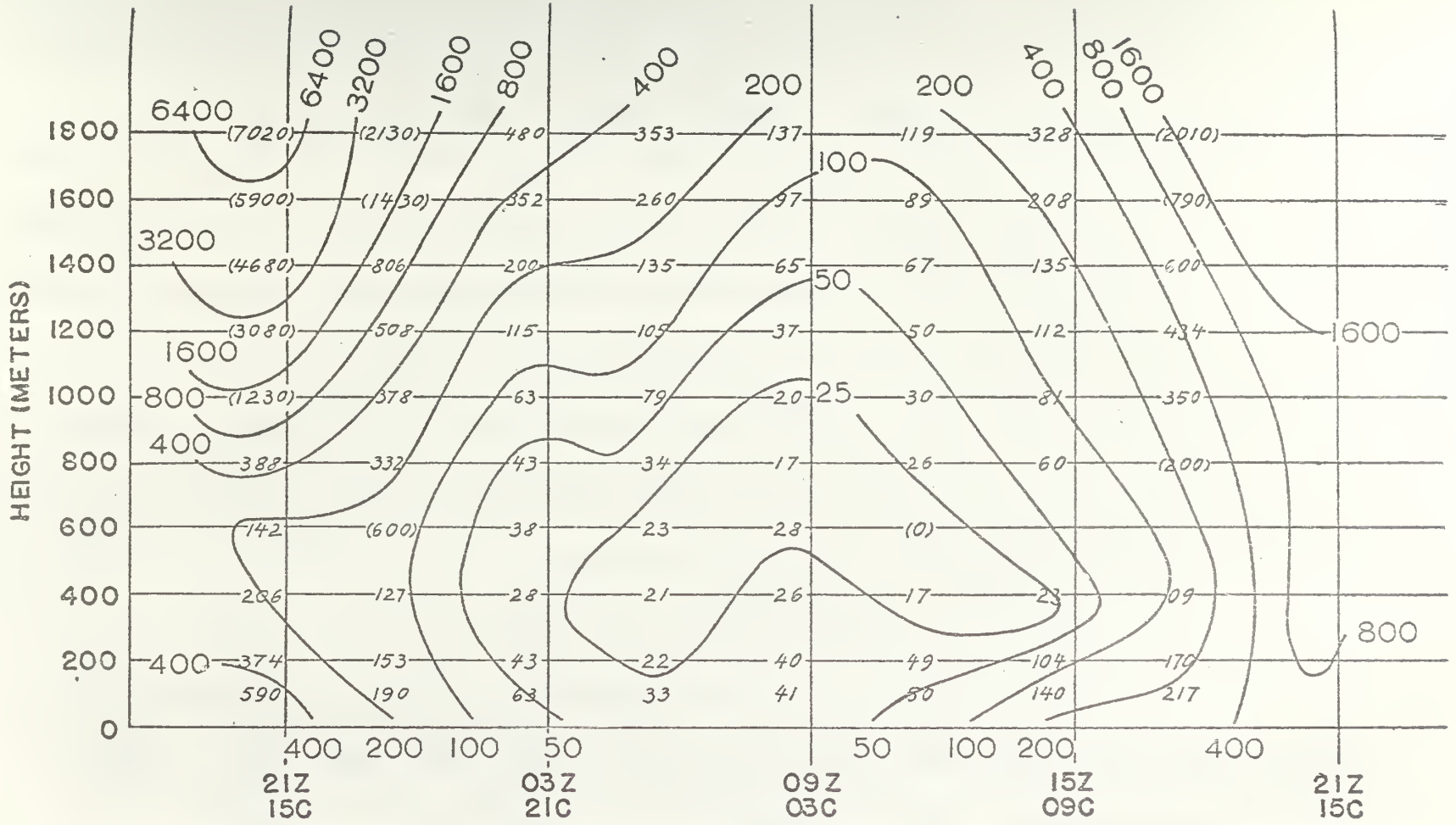

FIG. 3. Best estimate of the height-time distribution of eddy viscosity for the 24-day composite wind observations at Oklahoma City and Wichita, after Blackadar [1]

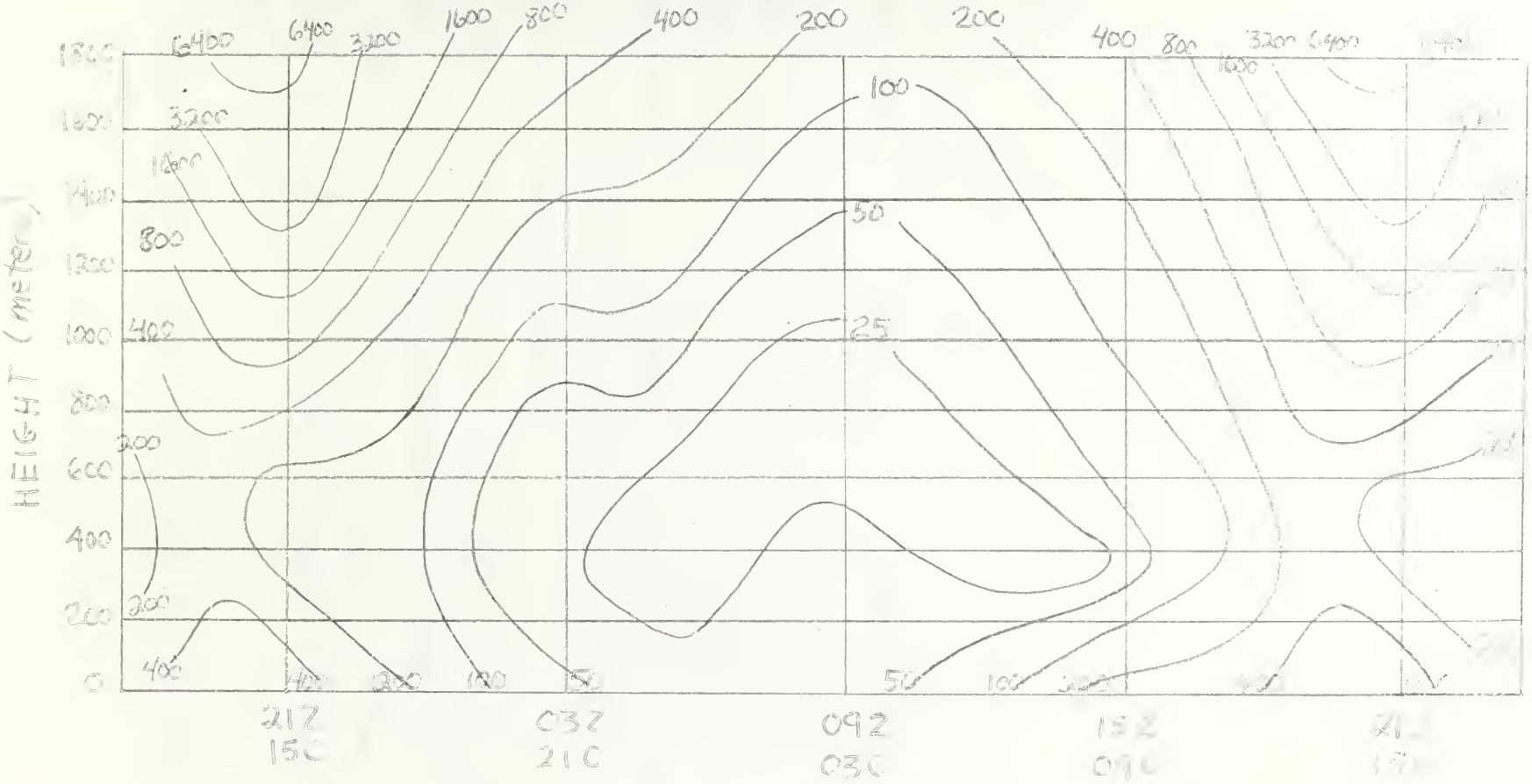

FIG. 4 Fig. 3 altered in the vicinity of 1500 CST

degrees. Now, having 10 equations of the same form as eq (4), fit a continuous function of z to the 10 values of A and T for each harmonic which makes a significant contribution. This would yield the final form of the equation.

$$\mathcal{M}(z,t) = A_0(z) + A_1(z) \cos\left[t + T_1(z)\right] + A_2(z) \cos\left[2t + T_2(z)\right] + \ldots\ldots A_6(z) \cos\left[6t + T_6(z)\right] \tag{5}$$

The harmonic analysis at each even 200 meter height was accomplished yielding the values in Table 1.

Fig. 5 shows values of A_0 (the mean), A_1 and A_2 versus height; fig. 6 shows A_3, A_4 and A_5 versus height. Fig. 7 shows T_1 and T_2 versus height and fig. 8 shows T_3, T_4 and T_5 versus height.

A diagonal difference table was computed for A_0 values versus height. The second differences of A_0, $\Delta^2 A_0$, showed the most nearly constant values. Although the second differences were not very close (ranging from 43 to 128), a parabola was fitted to the values of A_0 by the least squares method. As expected, the parabola did not fit the data to within sufficient accuracy.

Next it was noted from figs. 5 and 6 that a possible orderly decrease in the ratios of A_i/A_0 existed at each height as i increased from 1 to 5. A plot of the ratios A_i/A_0 versus height was drawn (see fig. 9). Utilizing these ratios the equation for $\mathcal{M}(z,t)$ would take on the form

$$\mathcal{M} = A_0(z)\left\{1 + B_1(z) \cos\left[t + T_1(z)\right] + B_2(z) \cos\left[(2t + T_2(z)\right] + \ldots\ldots B_6(z) \cos\left[(6t + T_6(z)\right]\right\} \tag{6}$$

TABLE 1.

Results of harmonic analysis at 10 levels.

Z is height above surface (m), A_0 the mean coefficient of eddy viscosity ($g\ cm^{-1}sec^{-1}$), A_i the amplitude of the i^{th} harmonic ($g\ cm^{-1}sec^{-1}$) and T_i is phase angle of i^{th} harmonic degrees. (1)

Z	A_0	A_1	T_1	A_2	T_2	A_3	T_3	A_4	T_4	A_5	T_5	A_6
0	204.1	233.4	26.1	86.2	40.2	40.0	38.7	22.9	54.9	7.6	96.8	2.6
200	118.3	138.8	19.7	74.8	34.9	35.6	61.2	24.4	83.7	19.4	125.8	8.8
400	75.8	87.8	12.9	54.3	31.9	24.8	69.1	16.6	115.5	18.5	156.0	9.3
600	87.0	103.5	13.7	50.0	34.5	19.4	69.4	15.3	123.8	23.7	165.1	12.2
800	144.3	191.9	11.9	98.7	27.6	45.8	43.7	18.5	106.5	26.0	152.2	14.4
1000	266	377.6	7.7	233.3	16.0	158.1	18.6	95.0	19.5	68.6	18.7	31.2
1200	461.2	690.0	3.3	471.5	8.2	351.1	8.3	248.4	6.5	196.6	6.9	93.7
1400	758	1162	2.2	806	7.1	560	8.3	360	8.0	258	8.0	114.6
1600	1160	1761	2.1	1169	8.6	756	11.8	438	15.6	266	15.2	105
1800	1690	2518	5.4	1620	18.1	984	31.0	539	44.0	249	45.5	60

(1) All surface values are the result of extrapolating Blackadar's [1] curves down to the surface.

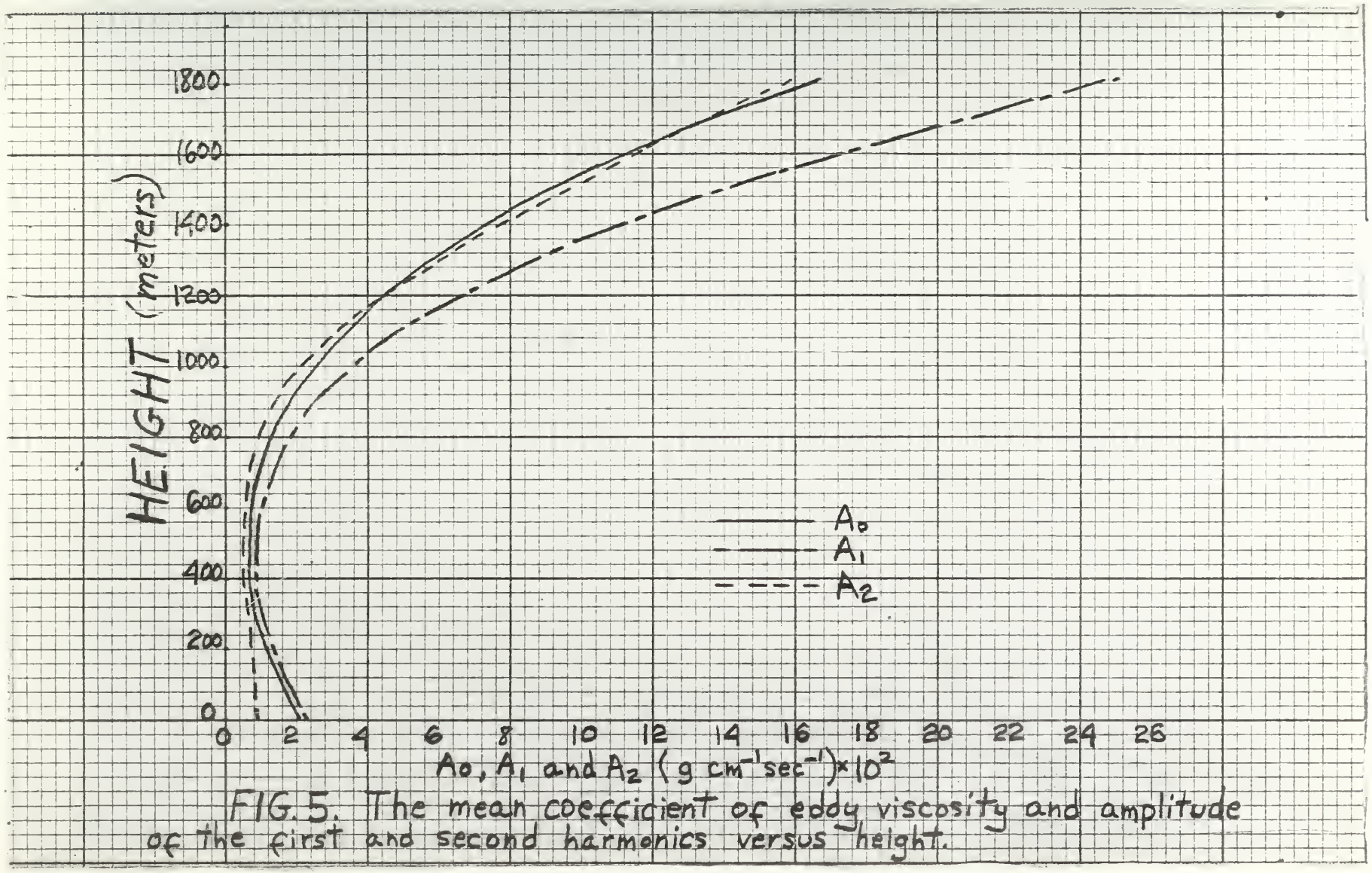

FIG. 5. The mean coefficient of eddy viscosity and amplitude of the first and second harmonics versus height.

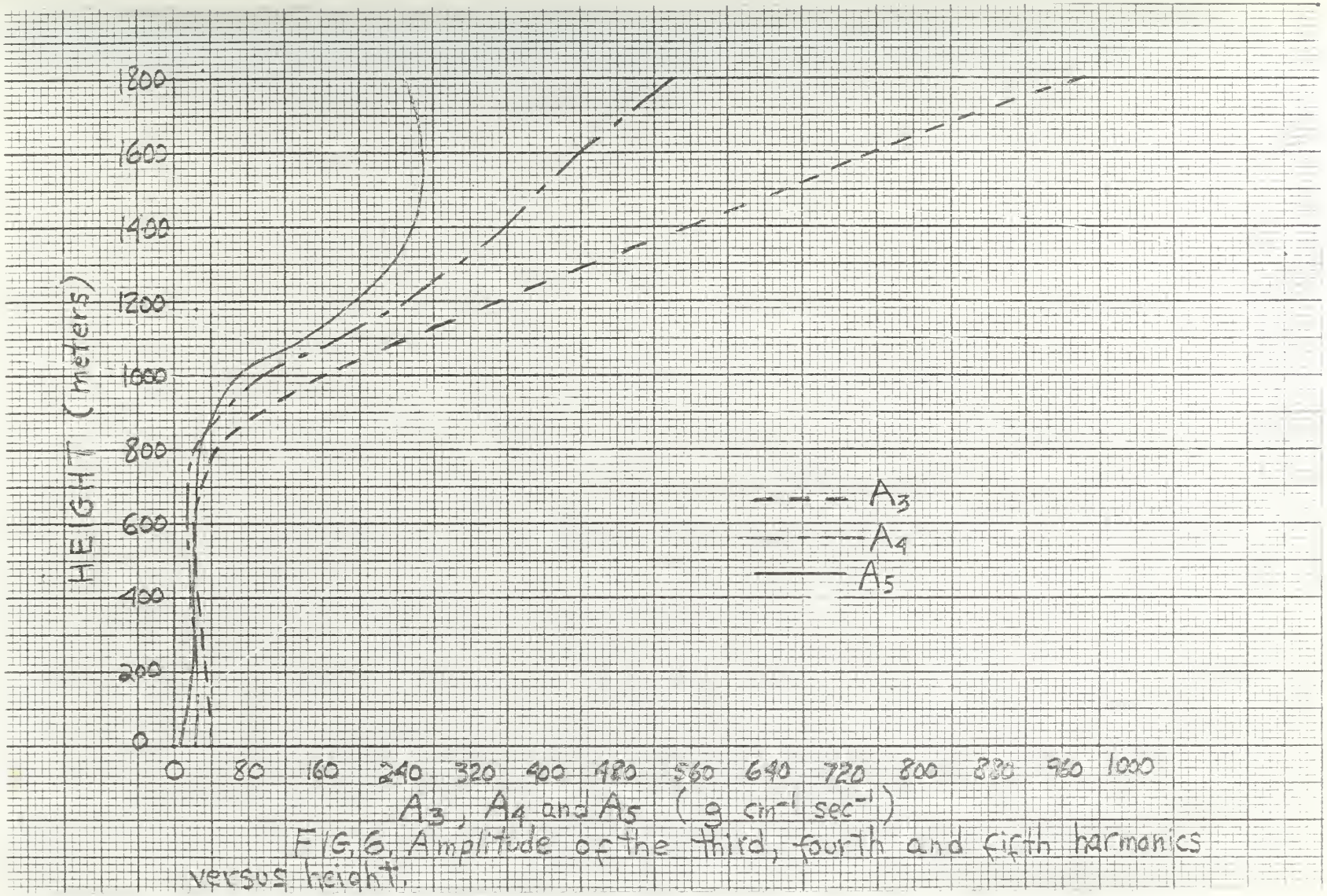

FIG. 6. Amplitude of the third, fourth and fifth harmonics versus height.

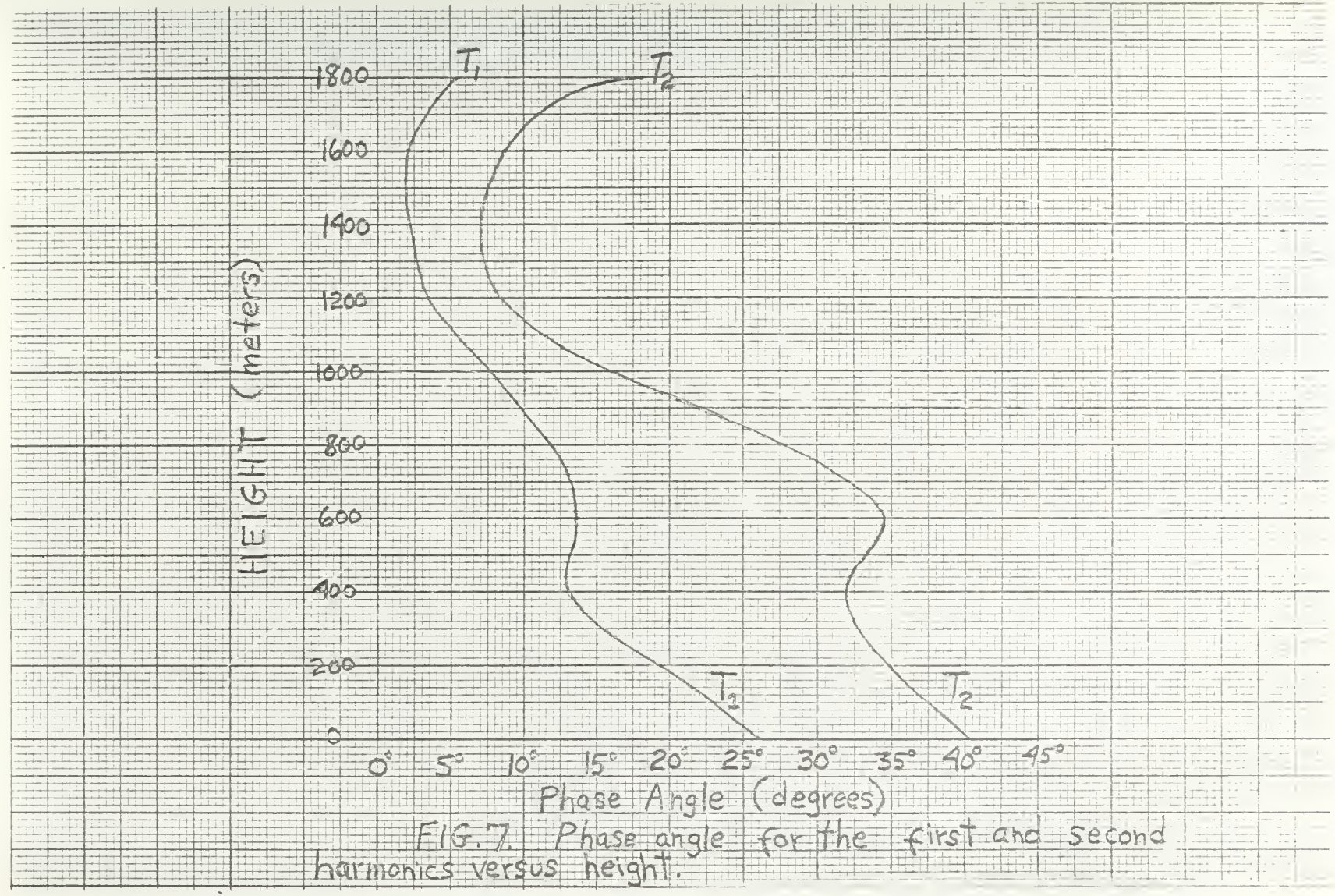

FIG. 7. Phase angle for the first and second harmonics versus height.

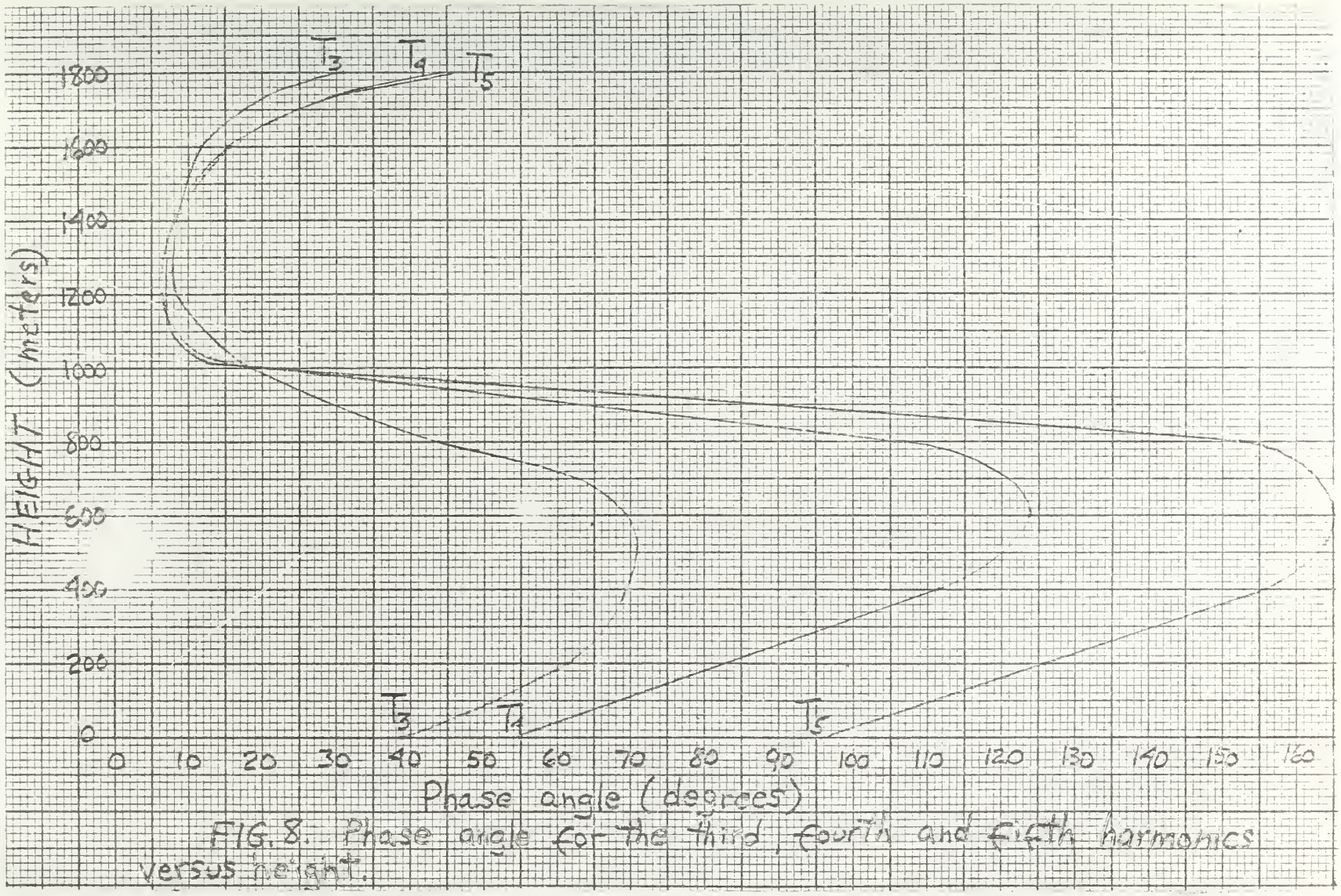

FIG. 8. Phase angle for the third, fourth and fifth harmonics versus height.

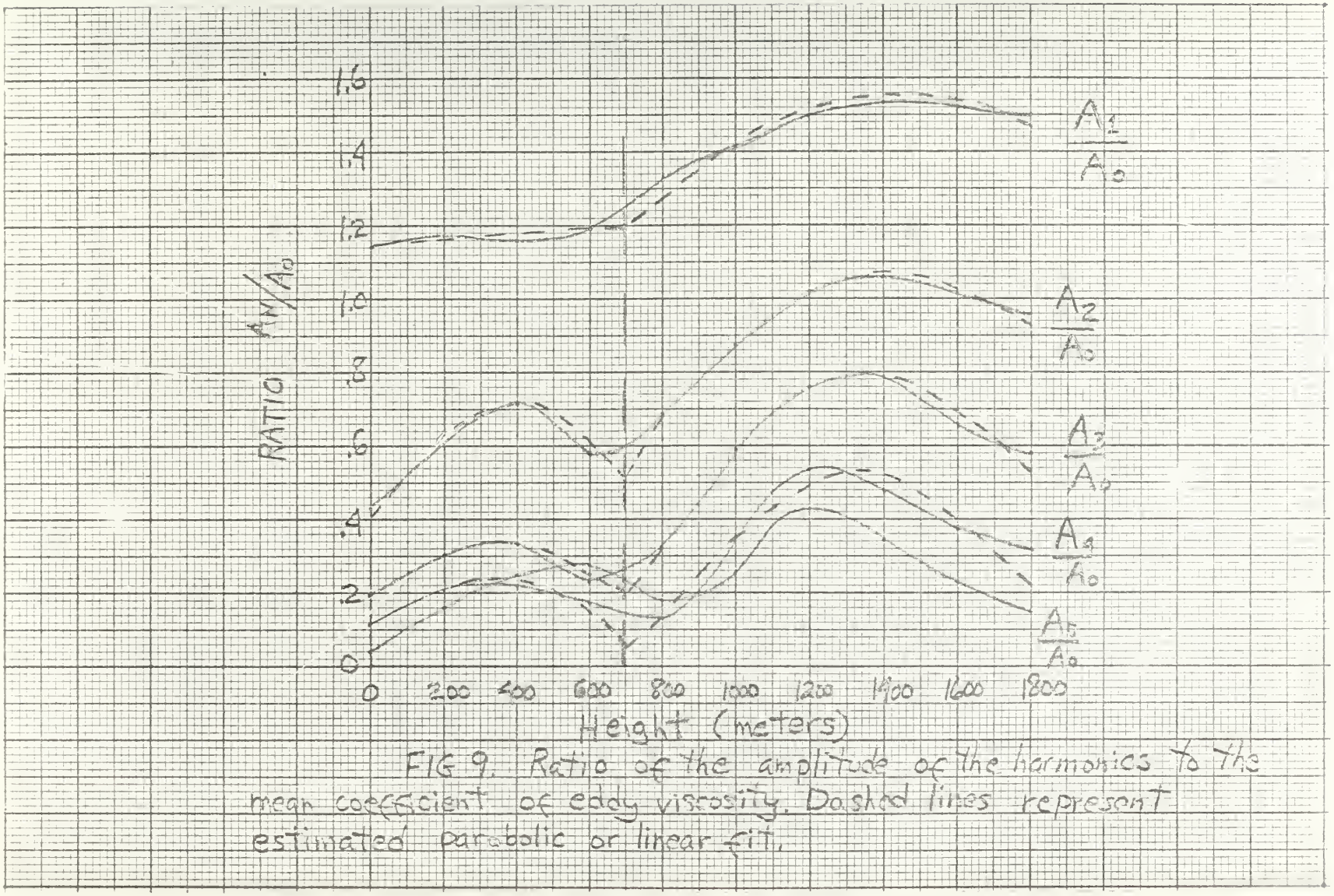

FIG 9. Ratio of the amplitude of the harmonics to the mean coefficient of eddy viscosity. Dashed lines represent estimated parabolic or linear fit.

Here $A_0(z)$ is the function of height needed to fit the observed values of the mean M at each height. $B_i(z)$ is the function of height needed to fit the ratio A_1/A_0 at each height and $T_i(z)$ is the function of height needed to fit the observed T_i values at each height. If the curves of fig. 9 could be fitted by a relatively simple function of height vice an estimated 5th or 6th degree polynomial, there existed a possibility of a series analysis and possible further simplification. One noteworthy aspect of this approach should be observed. It appears that a fairly simple function of height (e.g., a parabola) could be fitted to the ratio curves (fig. 9) with reasonable accuracy if a layerized approach is followed. The dashed lines on fig. 9 represent the probable curves which would fit a 2 layer model. The division of layers appears to be in the vicinity of 600 to 700 meters. This conceivably could be of physical significance.

Next it was noted that A_0 (fig. 5) increases non-linearly with height above 460 meters. Further, the point z = 460 meters, for which $A_0 = 73 g.cm^{-1}sec^{-1}$, appears to be a point of symmetry. The axis was translated to this point and A_0 versus height was plotted on log-log paper; this plot coincided almost exactly with a straight line. By the least squares method, $A_0(z) = az^n + b$ was determined. The equation for A_0 was

$$A_0(z) = 6.0 \left|z - 4.6\right|^{2.1} + 73 \qquad (7)$$

where z is height above the ground in hundreds of meters. Table 2 shows a comparison of the computed values of A_0 and observed values (from the harmonic analysis).

TABLE 2.

$A_0(z)$(g $cm^{-1}sec^{-1}$) computed versus $A_0(z)$ observed.

HEIGHT $Z_{meters} \times 10^{-2}$	COMPUTED $A_0(Z)$	OBSERVED $A_0(Z)$	PERCENT ERROR
0	225	204.	10.2
2	118.	118.	0.3
4	73.	75.	3.6
6	85.	87	2.0
8	153.	144.	6.3
10	286.	266	7.6
12	487.	461.	5.7
14	759.	758	0.2
16	1105	1160	4.7
18	1524	1690	9.8

Similarly $A_1(z)$ and $A_2(z)$ were obtained. A comparison of $A_1(z)$ computed and observed is shown in Table 3, and for $A_2(z)$ in Table 4. The equations developed by the least squares method are as follows:

$$A_1(z) = 8.4 \left| z - 4.5 \right|^{2.15} + 81 \tag{8}$$

$$A_2(z) = 2.5 \left| z - 4.0 \right|^{2.46} + 35 \tag{9}$$

When locating the approximate point of symmetry of the A_2 versus height curve (fig. 5), it was necessary to employ the method of least squares to determine which of three logically chosen positions for the height axis yielded the least difference between $A_2(z)$ calculated and $A_2(z)$ observed. In spite of this effort, relatively large differences were observed in the range, surface to 400 meters (see table 4), where the symmetry was weakest; however, the fit appears to e good above 600 meters.

A linear approximation was used to fit $T_1(z)$ and $T_2(z)$ (see fig. 7). The equations determined by the least squares method are

$$\begin{aligned} T_1(z) &= -1.20\ z + 21.4 \\ T_2(z) &= -1.81\ z + 39 \end{aligned} \tag{10}$$

where z = height above surface in hundreds of meters and $T_1(z)$ and $T_2(z)$ are in degrees. Table 5 shows a comparison of the phase angles computed by eq (10) for the first and second harmonics and the observed phase angles.

TABLE 3.

$A_1(z)$(g $cm^{-1}sec^{-1}$) computed versus $A_1(z)$ observed

HEIGHT $Z_{meters} \times 10^{-2}$	COMPUTED $A_1(Z)$	OBSERVED $A_1(Z)$	PERCENT ERROR
0	293.	233.	25.9
2	141.	139	1.7
4	81.	88.	7.6
6	103	103.	0.5
8	205	192	6.8
10	408.	377.	8.2
12	719.	690	4.3
14	1142	1162	1.7
16	1685	1761	4.3
18	2340	2518	7.1

TABLE 4.

$A_2(z)$(g $cm^{-1}sec^{-1}$) computed versus $A_2(z)$ observed

HEIGHT $Z_{meters} \times 10^{-2}$	COMPUTED $A_2(Z)$	OBSERVED $A_1(Z)$	PERCENT ERROR
0	110.	86.	27.6
2	48.	74.	34.9
4	35.	54.	35.5
6	48.	50.	2.6
8	110.	98.	11.8
10	239	233.	2.4
12	450.	471.	4.8
14	751.	806	6.8
16	1157	1169	1.0
18	1674	1620	3.3

TABLE 5.

$T_1(z)$ computed versus $T_1(z)$ observed

and $T_2(z)$ computed versus $T_2(z)$ observed for 10 levels.

$T_1(z)$ and $T_2(z)$ in degrees.

$Z_{meters} \times 10^{-2}$	$T_1(z)$obs.	$T_1(z)$comp.	$T_2(z)$obs.	$T_2(z)$comp.
0	26.	21.	40.	39
2	19.	18.	35	35.
4	13	16.5	32	32
6	14	14.1	34.	28.
8	12	12	27.	24.
10	7.	9.	16.	20.
12	3.	7	8.	17.
14	2.	4.	7.	13.
16	2.	2.0	8.	10.
18	5.	-0.4	18.	6.

Upon examination of the remaining amplitude coefficients and their corresponding phase angles (see figs. 6 and 8), it appeared that the functions of height needed to fit these values to the desired degree of accuracy would be relatively long and too complex to warrant further effort in this phase.

Also one of the objectives was to see how complicated a function of height and time it would take to yield the observed values of μ in fig. 3. The equation for $\mu(z,t)$ thus far obtained is

$$\mu(z,t) = 6.0 \left|z - 4.6\right|^{2.1} + 73 + \left[8.4 \left|z - 4.5\right|^{2.2} + 81\right] \cos\left[\frac{2\pi t}{24} + (21. - 1.2 z)\frac{\pi}{180}\right] + \left[2.4 \left|z - 4\right|^{2.5} + 35\right] \cos\left[\frac{2\pi t}{12} + (39 - 1.8 z)\frac{\pi}{180}\right] \quad (11)$$

where z = height above ground in meters x 10^{-2} and t is time in hours after t = 0 (1500 CST). Values of $\mu(z,t)$ were computed using the Marchant desk calculator for time intervals of one hour and every 100 meters height. Fig. 10 shows computed values of μ plotted on a height-time coordinate system.

Comparison of fig. 10 and the desired μ distribution from fig. 4, shows fig. 10 to contain a fairly representative set of isolines for μ from 1000 CST to 2000 CST from the surface to 1800 meters. Both figures show the largest order of magnitude for the coefficient of eddy viscosity at approximately 1500 CST at all levels. In addition, both figures show a minimum for μ in the vertical at approximately 400 meters between 1000 CST and 2000 CST with μ decreasing from the surface to 400 meters throughout the period and with μ increasing

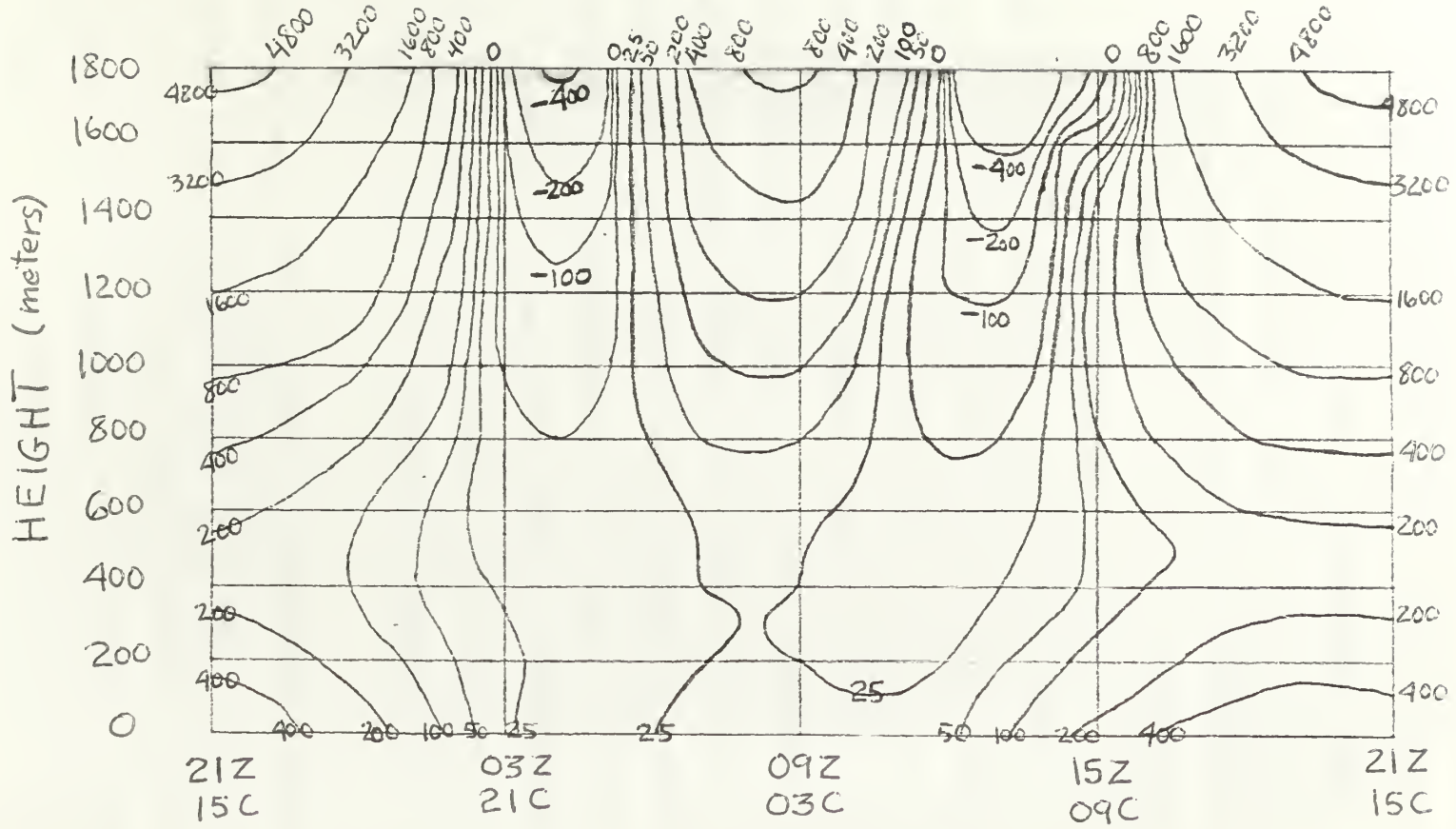

FIG.10. The coefficient of eddy viscosity distribution as a function of time and height as determined by the fitted mean and the first two harmonics.

rapidly with height above 400 meters from 1200 CST to 1800 CST. In fig. 10, however, the decrease of μ with time at any level above 1000 meters is too great in the vicinity of 1900 CST, as is the increase of μ with time too large at any level above 1000 meters in the vicinity of 1000 CST. Also, the vertical gradient of μ above 400 meters at 1500 CST is less than that observed on fig. 4. The latter could be rectified by computing the remaining harmonics which would tend to increase the values of μ computed at 1500 CST (t = 0) so that they more closely approach corresponding values of observed μ (fig. 10).

Between 2000 CST and 1000 CST, surface to 1800 meters, a comparison of fig. 4 and fig. 10 shows fig. 10 to have a completely unacceptable representation of the distribution of μ. Fig. 10 shows a column of minimum μ values extending vertically from the surface to 1800 meters at about 2200 CST, with no phase lag, and another minimum column, extending from the surface, at 0500 CST, to 1800 meters, where the minimum occurs at about 0700 CST. These minima are separated by a relatively strong maximum, surface to 1800 meters, occurring at 0200 CST. In contrast, the desired form, fig. 4, shows a strong single minimum extending from the surface, where it is estimated to occur at 2300 CST, to 1800 meters where it is observed at approximately 0500 CST.

The double maxima, double minima vice the desired single maximum, single minimum, are attributed primarily to the fact that the mean and only two of the six harmonics were utilized in deriving the values of μ for fig. 10. Fig. 11 is introduced to lend credence to the above remark. This figure shows the resultant of the first two harmonics versus time for height equal to 1200 meters. The resultant μ

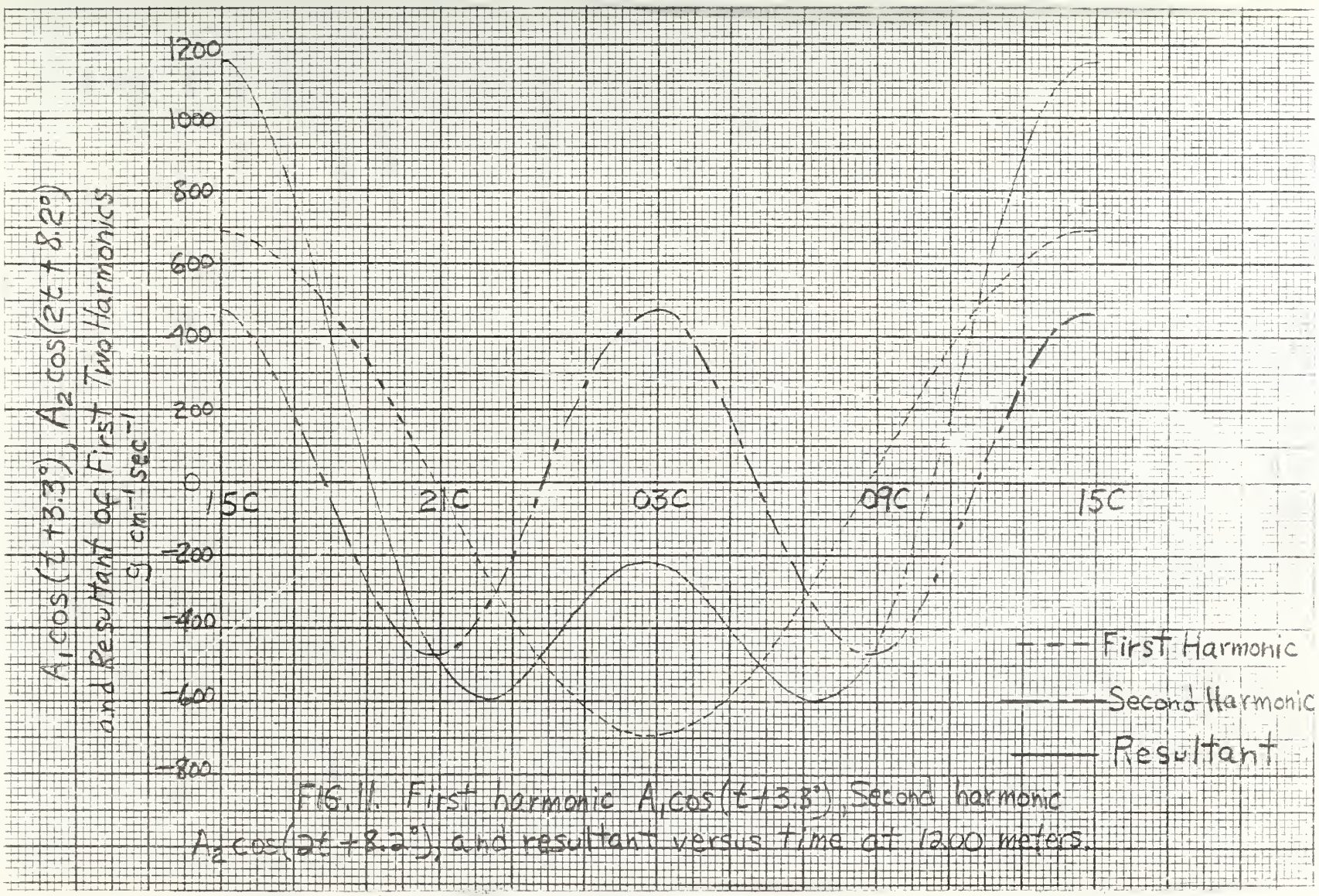

FIG. 11. First harmonic $A_1\cos(t+3.8°)$, Second harmonic $A_2\cos(2t+8.2°)$, and resultant versus time at 1200 meters.

distribution utilizing the mean and the first two harmonics as determined by the harmonic analysis, not from fitted values, tends to show the following characteristics: an absolute maximum at 1500 CST, a relative maximum at 0230 CST, and two minima, one at 0700 CST and the other at 2200 CST.

Each of the above maxima and minima are observed on fig. 10 at the corresponding times and the magnitude comparison is as follows:

TIME	μ from fig. 10	μ from fig. 11
1500 CST	1630	1620
2200 CST	-85	-140
0230 CST	213	240
0700 CST	-124	-140

Similar analysis at other heights would yield similar results.

This would tend to show then that the fitted values have not distorted the picture of μ distribution with time and height except to a slight degree and that the cause of the deviation of the computed μ values (fig. 10) from Blackadar's [1] observed values (altered fig. 4) must be the remaining four harmonics. Further, when using eq (11) and including the remaining four harmonics, the values of μ computed compare very favorably with the observed values.

Pertinent to the variation of μ with height, Estoque [3] has recently approximated the distribution of μ by a linear decrease of μ above a maximum μ value found at a height of about 50 meters. He proposes a two layer model for the frictional layer, the lower layer, called the surface sub-layer, extends to approximately 50 meters, and an upper layer, called the transition zone, extends to approximately 2000 meters. Utilizing this μ distribution, he has numerically integrated the equations of motion and heat conduction

equation to obtain the 24 hour distribution of wind and temperature. The diurnal wind distribution thus obtained by Estoque [3] appears to be in fairly good agreement with the diurnal wind characteristics observed on several occasions. However, for Blackadar's [1] data, (see fig. 3), it was necessary to attain an average height of approximately 1150 meters before μ varied linearly (but increased) with height to within a 10 percent error of the observed value of μ. Further, the slopes of the lines representing the linear variation of μ with height (for different times) varied up to 55°.

3. The Coefficient of Eddy Viscosity as a Function of Stability and Vertical Shear of the Wind.

Wind data for this phase were obtained from figs. 1 and 2, reproduced from Blackadar [1] . Temperature data for the 24 selected days were obtained from photo copies of WBAN-33 for the months of June, July, August, and September 1952 for Wichita, Kansas and Oklahoma City, Oklahoma, which were furnished by the National Weather Records Center, Ashville, North Carolina.

All temperatures at the reported levels (surface, 950, 900, 850, 800 and 750 mb) at both cities and at both sounding times (1500 GCT and 0300 GCT) were converted to potential temperature. The surface potential temperature was obtained by the Arowagram and upper level potential temperature was obtained from the Smithsonian Meteorological Tables.

For the 0300 GCT sounding and at each level, the average potential temperature was obtained by adding the 24 observations at Wichita to the 24 observations at Oklahoma City and dividing by 48. This yielded the average sounding for the two cities over the 24 day period at 0300 GCT. A similar procedure was followed to obtain the average height of the 950, 900, 850, 800 and 750 mb levels. All heights are in terms of 0.98 geodynamic meters. The same procedure was followed at 1500 GCT.

The average heights and potential temperatures obtained for the two times are shown in table 6. Next the stability factor ,

$$\frac{1}{\bar{\theta}} \frac{\partial \theta}{\partial z} \times 10^4$$

was computed for the center of the averaged layers using finite differences for the partial derivative of θ . Stability factor

TABLE 6.

Twenty four day average heights (in 0.98 geodynamic meters) and potential temperatures (degrees K) for the reported levels of concern.

	0300 GCT	
Level	$\bar{Z}$ meters	$\bar{\theta}$ degrees K
Surface	0	300.8
950mb	188	305.0
900mb	659.1	306.3
850mb	1156.3	307.6
800mb	1677	309.3
750mb	2228.2	311.9

	1500 GCT	
Level	$\bar{Z}$ meters	$\bar{\theta}$ degrees K
Surface	0	301.8
950mb	201	302.3
900mb	672.3	305.1
850mb	1168.2	307.0
800mb	1687.9	308.6
750mb	2237.6	310.7

versus height of center of layer for the two times is shown in table 7.

Values of the components of the vertical wind shear, $\frac{\partial u}{\partial z}$ and $\frac{\partial v}{\partial z}$, for each 100 meter level were then obtained from figs. 1 and 2 utilizing finite differences for the partial derivatives. The shear factor, $\left[\left(\frac{\partial u}{\partial z}\right)^2+\left(\frac{\partial v}{\partial z}\right)^2\right]10^6$, was computed next for each 100 meter level for the two times.

Graphs of μ observed versus the stability factor and of μ observed versus the shear factor were then constructed in an attempt to find a correlation between these factors and μ. One apparent correlation was that in the lower layers (below 600 meters) where pronounced stability variations occurred, strong stability was associated with a small μ, and vice versa. Above about 600 meters the contrast in stability factors was considered negligible. Moreover, there was insufficient difference between the μ values at each level for these two times (0900 CST and 2100 CST), nor between the shear factors in the upper levels (above 600 meters), to detect any correlation between wind shear and the values of μ observed. In the lower layers, when the shear appeared to be large, the value of μ was also large. In order to see if a correlation between wind shear and μ existed in the upper levels, it was necessary to examine the data at times of minimum and maximum μ (i.e. 0300 CST and 1500 CST). Computation of the required shear factors showed a strong correlation between low shear values and high μ values and vice versa for all levels. This did not contradict previous results above 600 meters but it was in opposition to the relationship found between shear and μ below 600 meters at 0900 and 2100 CST.

Since an expression throughout the vertical for μ in terms of stability and wind shear is a most desirable form, a compromise appeared

TABLE 7.

Stability factor, $\frac{1}{\theta}\frac{\partial\theta}{\partial z}\times 10^4$, versus height of center of layer for 24 day average soundings at 0300 GCT and 1500 GCT.

	0300 GCT			1500 GCT	
Layer	Height of center of layer (meters)	$\frac{1}{\theta}\frac{\partial\theta}{\partial z}\times 10^4$ (meters^{-1})	Layer	Height of center of layer (meters)	$\frac{1}{\theta}\frac{\partial\theta}{\partial z}\times 10^4$ (meters^{-1})
Surface to 950mb	94	.7498	Surface to 950mb	100	.0807
950mb to 900mb	424	.0826	950mb to 900mb	437	.1949
900mb to 850mb	908	.0865	900mb to 850mb	920	.1265
850mb to 800mb	1417	.1065	850mb to 800mb	1428	.0969
800mb to 750mb	1953	.131	800mb to 750mb	1963	.1250

to be necessary, i.e., a two layer model with μ a function of the stability factor below 600 meters and μ a function of the shear factor above 600 meters. Now, from visual inspection of figs. 1 and 2 at 1500 CST and from prior shear computations the shear can be seen to be very small and practically constant throughout the layer surface to 1800 meters; yet the value of μ (see fig. 3) increases rapidly from 600 meters upwards. Therefore, a second compromise from the originally intended solution appeared to be in order, i.e., above 600 meters let μ vary with the shear factor and with height. Further, due to the lack of temperature data below 600 meters, it was decided to utilize the mean μ (z) with respect to time in an attempt to more accurately describe the μ observed values and also perhaps to extend the coverage below 600 meters to the entire 24 hour period rather than merely the times of the two temperature soundings.

The general approach used in the solution of the problem is as follows:

1) Assume (for both layers)

$$\mu = \overline{\mu}_{(z)} + \Delta\mu \tag{12}$$

where μ is the observed value of μ for any point in time and space, $\overline{\mu}$ (z) is the mean value of all μ observed at the level z, and $\Delta\mu$ is the difference between the observed value of μ and the mean value of μ at that height.

2) Find the best function of height which yields the $\overline{\mu}$ (z) distribution.

3) Account for $\Delta\mu$, the deviation from the mean,

a) below 600 meters by a function of stability factor,
b) above 600 meters by a function of shear factor.

A function was found in Section 2 to represent the mean μ at any height (see eq (7)); however, this was based upon values obtained from the isolines of μ in fig. 4. For this section an attempt was being made to find the function which yielded the computed values plotted on fig. 3, inasmuch as they were in part computed from the vertical shear of the horizontal wind. A similar approach to that used in deriving eq (7) was in order and yielded the following for $\overline{\mu}(z)$

$$\overline{\mu}(z) = 5.6 \left| z - 4.8 \right|^{2.2} + 65 \qquad (13)$$

where z is height above the ground in hundreds of meters. Due to the relatively good fit, this equation was taken to apply in both layers.

Next $\Delta\mu$ values were computed by subtracting the $\overline{\mu}(z)$ values computed with eq (13) from the values of μ observed on fig. 3.

A plot of $\Delta\mu$ versus stability factor is shown as fig. 12. Four of the points plotted are from observed data for the period (table 7) and the fifth point is an estimated value for a height of 150 meters at 1500 CST. This value was derived from 12 soundings taken during the Great Plains Turbulence Field Program [5] in August and September 1953 and under similar atmospheric flow conditions. The stability factor obtained was .0035 m^{-1}, and the $\Delta\mu$ corresponding to 1500 CST and 150 meters is 340 g $cm^{-1} sec^{-1}$. The curve appearing on the figure has been faired in and does not represent the fitted function given below.

Of various functions of the stability factor tried, that which yielded the smallest "least squares" error for $\Delta\mu$ was the hyperbola,

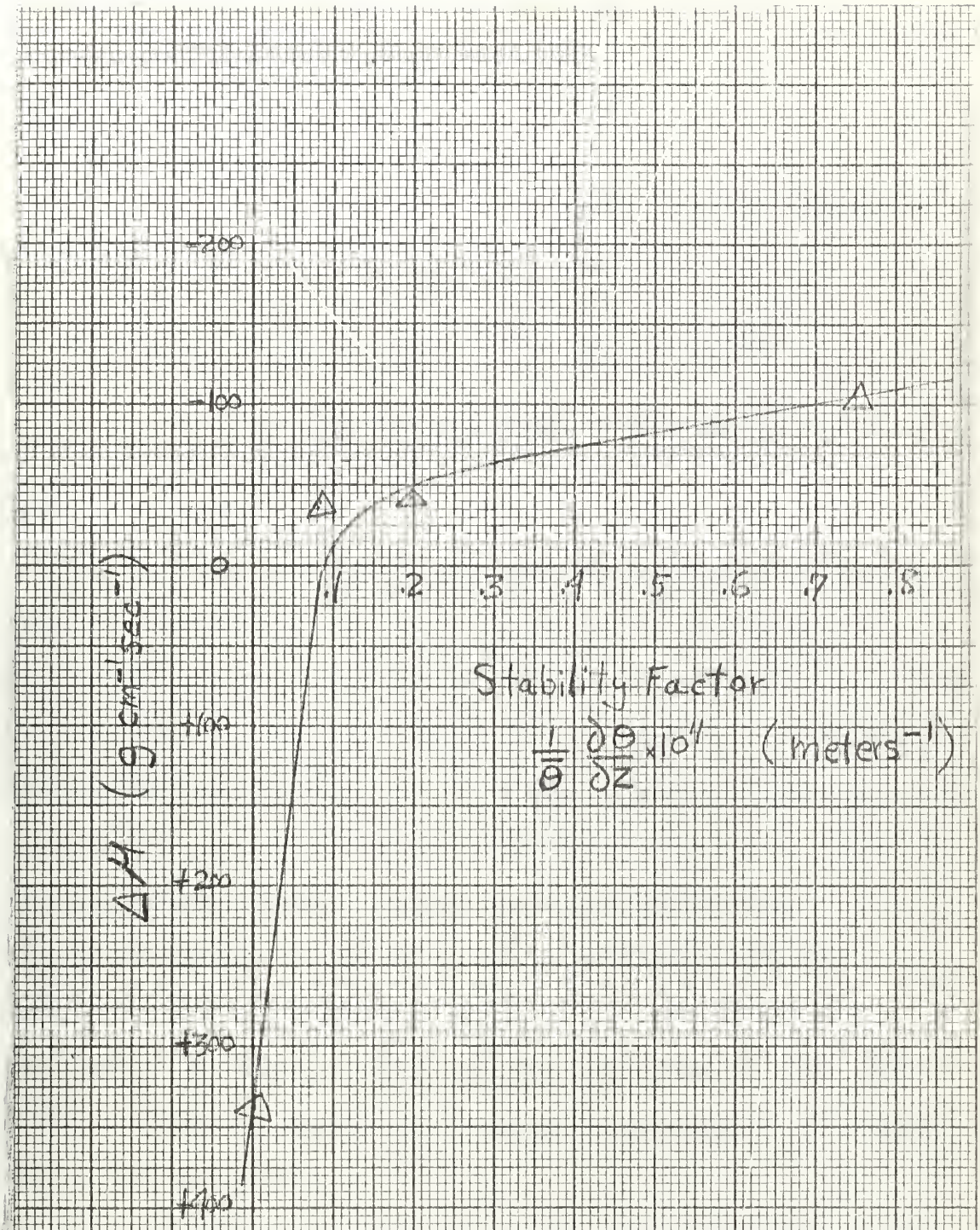

FIG. 12. Deviation of the observed eddy viscosity from the mean versus stability factor.

$$\Delta\mu = 121 - 5 (S_\theta) + \tfrac{1}{2}\left[200{,}500 - 7400(S_\theta) + 123 (S_\theta)^2\right]^{\frac{1}{2}}$$

where $(S_\theta) = \frac{1}{\theta}\frac{\partial\theta}{\partial z} \times 10^7 (m^{-1})$. (14)

Combining eq (13) and eq (14) then yields the desired form for computing μ, i.e.

$$\mu \text{ computed} = 5.60\left| z - 4.8\right|^{2.20} + 186 - 5.6 (S_\theta) + \tfrac{1}{2}\left[200{,}500 - 7400(S_\theta) + 123 (S_\theta)^2\right]^{\frac{1}{2}} \quad (15)$$

Here z is in meters x 10^{-2}.

Table 8 shows a comparison of μ computed and μ observed for the layer below 600 meters. The largest error occurs at 2100 CST and a height of 424 meters. It should be noted (see figs. 1, 2) that at this point the shear is relatively strong which, according to eq (3), would tend to yield a small value for μ. A similar analysis applies for the next largest error, percentwise, at 0900 CST and 437 meters. Here, where the observed value is greater than the computed value, a low value of wind shear is observed. From the preceding analysis, it appears that shear is becoming a factor in the upper levels of the lower layer. In this transition zone from approximately 400 to 600 meters, a better representation of μ might be obtained by considering shear as well as stability.

For the layer above 600 meters, a graph was drawn showing height versus shear factor and the associated $\Delta\mu$ value (next to each point) needed to yield the observed value of μ for the four times shear computations were made. This is shown as fig. 13.

TABLE 8.

Comparison of μ computed and μ observed(g $cm^{-1} sec^{-1}$), surface to 600 meters.

Time (CST)	Height above Surface (meters)	μ observed g $cm^{-1} sec^{-1}$	μ computed g $cm^{-1} sec^{-1}$
2100	94	60	60
2100	424	27	49
0900	100	140	155
0900	437	24	16
1500	150	480	460

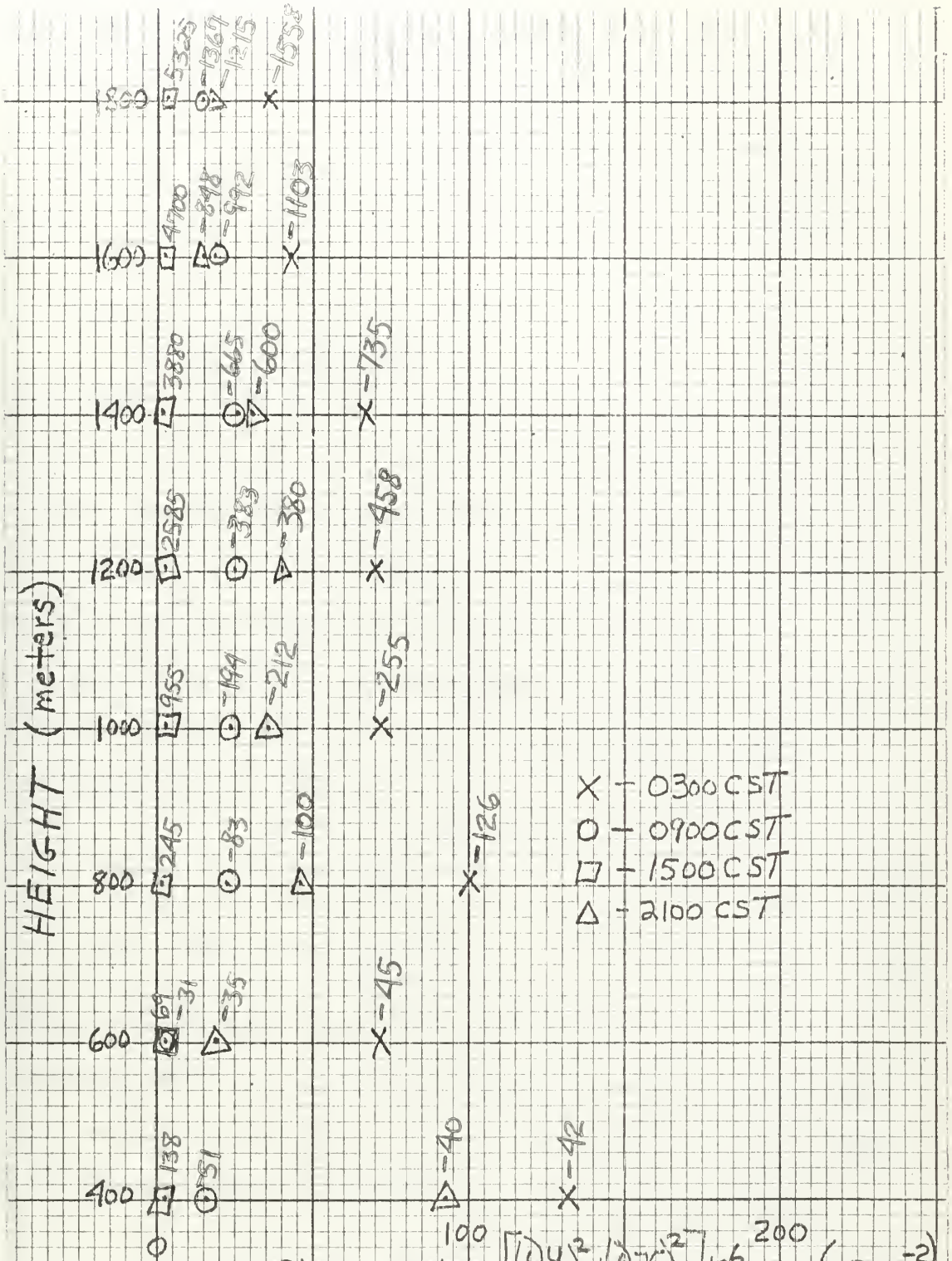

FIG. 13. Height versus shear factor and deviation from the mean for four times ($\Delta\mu$ recorded alongside each point.

As previously stated it was desired to account for $\Delta\mu$ values as a function of height and shear. The approach to the problem was similar to that used in section 2. An equilateral hyperbola was fitted to the observed values of shear and $\Delta\mu$ at each level (600, 800, 1000 ....1800 meters) to provide the $\Delta\mu$ distribution as a function of shear factor. The result is

$$\Delta\mu_z = \frac{c_z}{\left[\left(\frac{\partial u}{\partial z}\right)^2 + \left(\frac{\partial v}{\partial z}\right)^2\right] \times 10^6} + b_z \qquad (16)$$

where $\Delta\mu z$ is the difference between the observed μ and $\overline{\mu}(z)$ at height z above the ground; c_z and b_z are the constants determined by the least squares method at the z level. Fig. 14 shows c_z and b_z versus height. The curves appearing on the figure have been faired in and do not represent the fitted function given below.

Next the c_z and b_z values determined at each height were fitted with a continuous function of height. The functions of height representing each of these is

$$c(z) = .22 \quad (z)^{4.} \qquad (17)$$

$$b(z) = .10 \quad z)^{3.5} \qquad (18)$$

where z is height above ground in meters x 10^{-2}.

A comparison of the c_z and b_z values observed and the c(z) and b(z) values computed is shown in table 9. The resulting function of shear and height representing the $\Delta\mu$ values at 600 meters and above is

$$\Delta\mu = \frac{.22 \quad (z)^4}{\left[\left(\frac{\partial u}{\partial z}\right)^2 + \left(\frac{\partial v}{\partial z}\right)^2\right] \times 10^6} - (.1) \quad (z)^{3.5} \qquad (19)$$

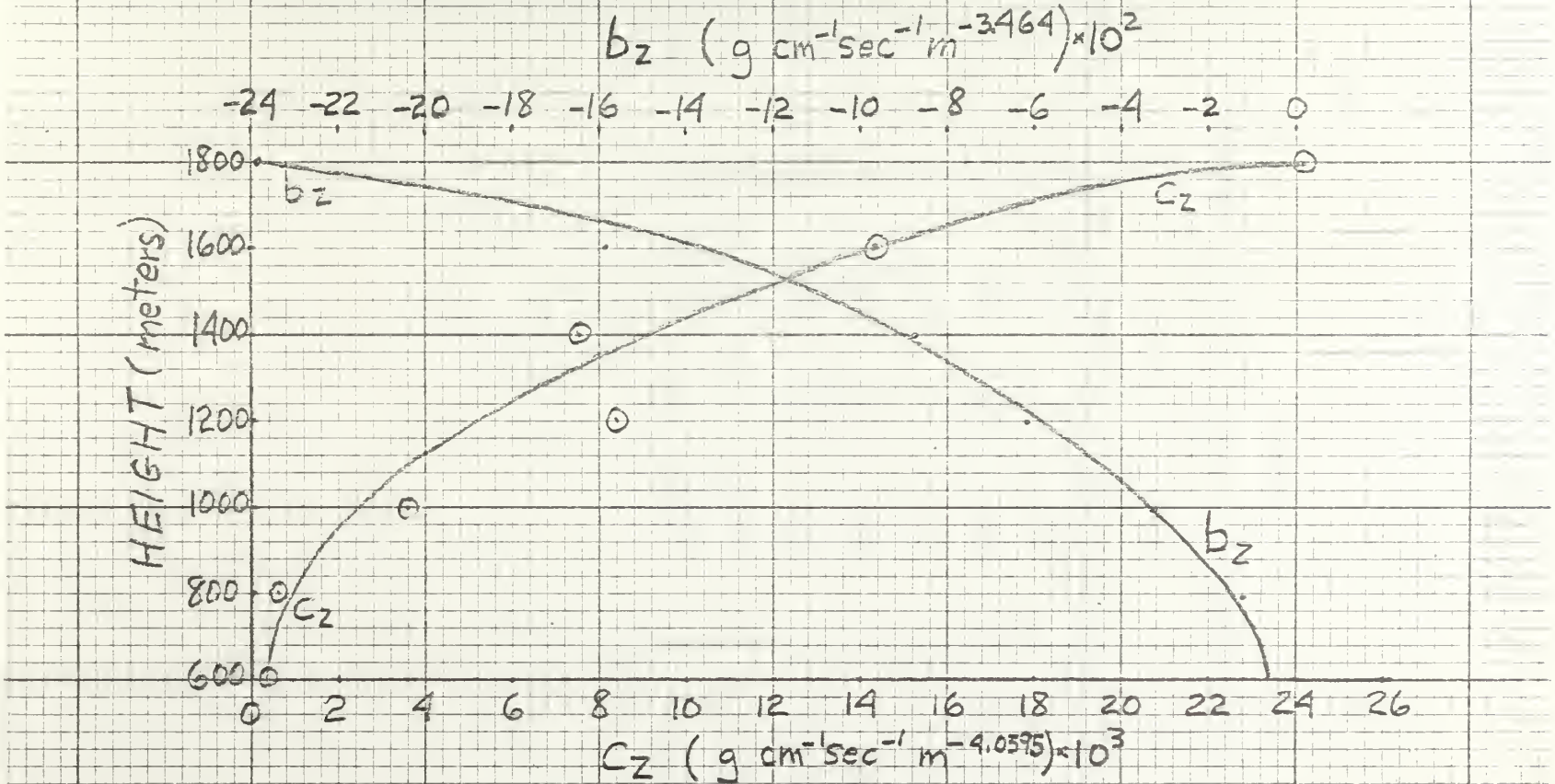

FIG. 14. The coefficients C_z and b_z versus height.

TABLE 9.

The constants c_z and b_z versus c(z) and b(z) at each level.

z meters $\times 10^{-2}$	c_z g $cm^{-1}sec^{-3}$	c(z) g $cm^{-1}sec^{-3}$	b_z $cm^{-1}sec^{-1}$	b(z) g $cm^{-1}sec^{-1}$
6	314	309	-56	-51
8	623	982	-119	-140
10	3604	2440	-320	-302
12	8396	4980	-609	-574
14	7457	9381	-870	-970
16	14,372	16,115	-1590	-1541
18	24,147	25,840	-2378	-2318

and the function representing μ in the upper layer is

$$\mu = 5.6 \quad (z - 4.8)^{2.2} \quad 65 + \frac{.22 \quad (z)^{4.0}}{\left[\left(\frac{\partial u}{\partial z}\right)^2 + \left(\frac{\partial v}{\partial z}\right)^2\right] \times 10^6} - (.1)(z)^3 \tag{20}$$

A comparison of the computed μ values and the observed values is shown in Table 10.

The distribution of μ computed indicated in Table 10 compares fairly well with the observed values. The salient features of the observed μ distribution are preserved by the computed pattern, i.e., a maximum at each level at time 1500 CST (one exception at 600 meters) and a minimum at each level at time 0300 CST. In most instances the order of magnitude of the observed and computed values are the same (five exceptions out of 28 observations). The value observed at 0900 CST, height 600 meters, is approximately one fifth that computed by shear and height function. This discrepancy may partially be accounted for by the higher stability factor observed in the vicinity (see table 7). The negative values computed for heights 1200 and 1400 meters at 0300 CST are primarily a result of the curve fitting process. (See fig. 14 and table 9).

TABLE 10

Comparison of computed coefficient of eddy viscosity, μ_c (g $cm^{-1} sec^{-1}$) and observed, μ_o for four times in upper layer.

Height (meters)	μ_c	(μ_o)	μ_c	(μ_o)	μ_c	(μ_o)	μ_c	(μ_o)
1800	7607	(7020)	455	(480)	105	(137)	1100	(328)
1600	6709	(5900)	734	(352)	36	(97)	509	(208)
1400	5800	(4680)	142	(200)	-29	(65)	177	(135)
1200	1811	(3080)	44	(115)	-7	(37)	120	(112)
1000	836	(1230)	41	(63)	7	(20)	75	(81)
800	577	(388)	24	(43)	13	(17)	46	(60)
600	99	(142)	48	(38)	26	(28)	228	(42)

21Z 03Z 09Z 15Z

15C 21C 03C 09C

4. Conclusions.

From the approach followed in this investigation a simple representation of the diurnal variation of the coefficient of eddy viscosity with height was not apparent.

It has been shown that the function of height and time representing the mean and first two harmonics is inadequate to show the salient features of the observed distribution.

In order to represent the observed distribution of the coefficient of eddy viscosity by a function of height and time, it would take a relatively long series of terms, estimated to encompass at least five harmonics, involving exponential functions of height, fourth or fifth degree polynomial functions of height, and trigonometric functions of angles dependent on time and functions of height.

A two layer model is developed in an attempt to account for the observed distribution of the coefficient of eddy viscosity as a function of stability and shear of the wind. It is found useful in the lower layer, and essential in the upper layer, to include height above the ground as one of the parameters determining the distribution. The variance of the coefficient with stability in the lower layer appears well founded, as does that between shear and the eddy viscosity coefficient in the upper layer; consequently, a fair representation of the general characteristics of the observed diurnal variation of the coefficient of eddy viscosity is obtained from the empirical formulae representing the two layers.

Further investigation utilizing more frequent and detailed wind and temperature observations would be likely to yield better results and might eliminate the need for the two layer approach.

5. Bibliography.

1. Blackadar, A. K., Final Report on Study of Forecasting Low-level Wind Gradients, AFCRC - TR - 59220, ASTIA AD 211358, Pennsylvania State University, 1959

2. Buajitti, K. and Blackadar, A. K., Theoretical Studies of diurnal wind-structure variations in the planetary boundary layer, Quarterly Journal of the Royal Meteorology Society, Vol. 83, No. 358, pp 486-500, 1957

3. Estoque, M. A., A Preliminary Report on a Boundary Layer Numerical Experiment, AFCRC - TN - 59 - 462, GRD Research Notes No. 20, 1959

4. Haltiner, G. J., The Diurnal Variation of the Wind, Tellus XI, 4 1959

5. Lettau, H. H. and Davidson, B., Exploring the Atmosphere's First Mile, Pergamon Press, 1957

6. Mildner, P., Beitr. phys. frei Atmos., vol 19, 1932